J. Fluid Mech. (1988), *vol.* 186, *pp.* 501–520
Printed in Great Britain

Current effects on resonant reflection of surface water waves by sand bars

By JAMES T. KIRBY

Coastal and Oceanographic Engineering Department, University of Florida, Gainesville, FL 32611, USA

(Received 3 March 1987 and in revised form 23 June 1987)

The effect of currents flowing across a bar field on resonant reflection of surface waves by the bars is investigated. Using a multiple-scale expansion, evolution equations for the amplitudes of linear waves are derived and used to investigate the reflection of periodic wave trains with steady amplitude for both normal and oblique incidence. The presence of a current is found to shift resonant frequencies by possibly significant amounts and is also found to enhance reflection of waves by bar fields due to the additional effect of the perturbed current field.

1. Introduction

The possibility of obtaining strong reflections of incident surface water waves through interaction with undular topography has drawn attention in recent years to the mechanism's possible impact on coastal geomorphology. Davies & Heathershaw (1984) have investigated bottom topographies of the form

$$h(x) = \bar{h} + \delta(x), \tag{1.1}$$

where $h(x)$ denotes total water depth, $\bar{h}$ represents a steady mean depth and $\delta(x)$ represents a small-amplitude, rapid perturbation. 'Small amplitude' implies $|k\delta| \ll 1$ in general scaling or $|\delta/h| \ll 1$ in shallow-water scaling. In experiments to date, $\delta(x)$ has been given the simple form

$$\delta(x) = D \sin \lambda x; \quad 0 \leqslant x \leqslant L. \tag{1.2}$$

This represents a long-crested bar field confined in the region $\{0 \leqslant x \leqslant L\}$ consisting of n bars, with uniform bar amplitude D and bar wavenumber λ constrained according to $\lambda = 2\pi n/L$. The sinusoidal form is convenient in that it is physically plausible and contributes only a single wave-like perturbation in the mathematical analysis. Davies & Heathershaw experimented with normally incident waves of variable wavenumber–frequency $\{k, \omega\}$ and clearly demonstrated a strong resonance in the neighbourhood of $2k/\lambda = 1$, leading to greatly enhanced reflection. They pointed out the analogy between this resonance and Bragg-scattering in crystallography, but provided an analysis only for the case of weak reflection. Their analysis, done in the context of regular perturbations, breaks down at the resonance condition.

Mei (1985) examined the neighbourhood of the resonance directly using a resonant-interaction analysis and obtained good predictions of the maximum reflections observed in Davies & Heathershaw's experiments. Mei also examined the case of detuned interaction, where wave frequency ω is allowed to deviate from resonant frequency ω_0 by an amount Ω. No direct comparison was made between the

predictions for detuned waves and data. Kirby (1986) provided an extension of the mild-slope equation to handle the general case of arbitrarily varying $\delta(x, y)$ on a slowly varying mean depth $\bar{h}(x, y)$. Numerical simulation of Davies & Heathershaw's experiments also provided good reproduction of measured reflection coefficients. Hara & Mei (1987) have extended the resonant-interaction theory to second order in $|\delta|$ and have performed additional experiments which illustrate the existence of a cutoff condition for frequency Ω, which is explained further below.

The existence of the Bragg scattering mechanism provides a possible means for constructing coastal protection devices which are relatively low in profile in comparison to local water depth. The installation of such an artificial bar field fronting a beach may provide a means for significantly reducing wave energy arriving at the surf zone. Given that any such installation would necessarily be of finite extent in the longshore direction, it is likely that the resulting localized depression in maximum set-up behind the bar field would generate a nearshore circulation pattern. Prediction of such a pattern depends on future hydrodynamic modelling. However, its result would be to introduce onshore or (more likely) offshore flows over the bar field. In order to evaluate the effectiveness of the bar field in the presence of an induced circulation, it is necessary to understand the effect of wave–current interaction over the bar field.

In this study, we examine the reduced case of the propagation of waves over a bar field $\delta(x)$ resting on an otherwise flat bottom $z = -h$. Not accounting for the bar-field perturbation, the current field $\{U_0, V_0\}$ is taken to be constant and of the order of linear wave phase speed (e.g. $O(1)$) in the perturbation analysis. In §2, we state the full problem and then give the solutions for the steady flow to $O(\delta)$, following Kennedy (1963) and Reynolds (1965). Then, in §3, we examine the current's effect on the conditions for Bragg resonance. The evolution equations for the linear wave scattering problem are constructed in §4. Solutions and various examples for normal wave incidence are examined in §5. Finally, in §6 we provide sufficient information to construct the similar solutions for the oblique-incidence case.

2. Solution for the perturbed mean flow

We first solve for the flow field and surface displacement resulting from the interaction of a uniform flow $\{U_0, V_0\}$ and bottom displacement $\delta(x)$ given by (1.2). Figure 1 illustrates the various quantities described below. The full problem for waves and current may be written in terms of surface displacement η and velocity potential ϕ according to

$$\nabla_h^2 \phi + \phi_{zz} = 0, \qquad -h \leqslant z \leqslant \eta, \tag{2.1a}$$

$$\phi_z = \epsilon \nabla_h \cdot \{\delta \nabla_h \phi\}, \qquad z = -h, \tag{2.1b}$$

$$g\eta + \phi_t + \tfrac{1}{2}(\nabla_h \phi)^2 + \tfrac{1}{2}(\phi_z)^2 = c(t), \qquad z = \eta, \tag{2.1c}$$

$$\eta_t + \nabla_h \phi \cdot \nabla_h \eta = \phi_z, \qquad z = \eta, \tag{2.1d}$$

where ϵ denotes the effect of the small bottom perturbation. Noting that only linear wave motion is to be considered, we may split ϕ, η and c into time-steady parts associated with the current and time-harmonic parts associated with the waves:

$$\phi = \phi_c + \phi_w; \quad \eta = b + \eta_w; \quad c = c_c + c_w. \tag{2.2a, b, c}$$

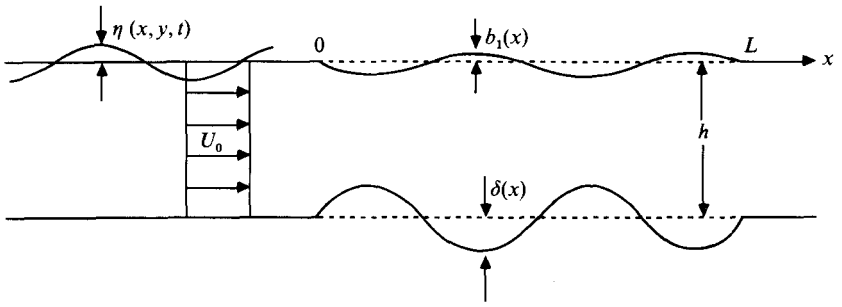

FIGURE 1. Definition sketch.

Substituting (2.2) in (2.1) and isolating time-steady terms yields

$$\nabla_h^2 \phi_c + \phi_{c,zz} = 0, \qquad -h \leqslant z \leqslant b, \tag{2.3a}$$

$$\phi_{c,z} = \epsilon \nabla_h \cdot (\delta \nabla_h \phi_c), \qquad z = -h, \tag{2.3b}$$

$$gb + \tfrac{1}{2}(\nabla_h \phi_c)^2 + \tfrac{1}{2}(\phi_{c,z})^2 = c_c, \qquad z = b, \tag{2.3c}$$

$$\nabla_h \phi_c \cdot \nabla_h b = \phi_{c,z}, \qquad z = b. \tag{2.3d}$$

We now introduce the expansion

$$\phi_c = \phi_{0c} + \epsilon \phi_{1c}, \tag{2.4a}$$

$$b = b_0 + \epsilon b_1, \tag{2.4b}$$

$$c = c_0 + \epsilon c_1. \tag{2.4c}$$

At $O(1)$ we obtain the solution for the undisturbed current field:

$$\phi_{0c} = (U_0 x + V_0 y), \tag{2.5}$$

$$b_0 = 0, \tag{2.6}$$

$$c_0 = \tfrac{1}{2}(U_0^2 + V_0^2), \tag{2.7}$$

where c_0 is chosen so as to render the $O(1)$ depth equal to h. We define Froude numbers associated with the horizontal currents according to

$$F_x = \frac{U_0}{(gh)^{\frac{1}{2}}}; \quad F_y = \frac{V_0}{(gh)^{\frac{1}{2}}}. \tag{2.8}$$

At $O(\epsilon)$, we obtain the problem considered by Kennedy (1963) and Reynolds (1965), restricted here to the case of time-steady bottoms. The solution to that problem is given by

$$\phi_{1c} = \frac{U_0 D}{2\alpha} \{\beta \cosh \lambda(h+z) + \alpha \sinh \lambda(h+z)\} e^{i\lambda x} + \text{c.c.}, \tag{2.9}$$

$$b_1 = \frac{-i\lambda h F_x^2 D}{2\alpha \cosh \lambda h} e^{i\lambda x} + \text{c.c.}, \tag{2.10}$$

where

$$\alpha = \lambda h F_x^2 - \tanh \lambda h, \tag{2.11a}$$

$$\beta = 1 - \lambda h F_x^2 \tanh \lambda h. \tag{2.11b}$$

The perturbed flow field has a singularity at the zero of α, which corresponds to the dispersion relation for a steady wave of wavenumber λ riding on current U_0. The singularity is thus due to a resonance of the free wave by the bottom forcing. Mei (1969) has shown that this singularity may be removed in a higher-order nonlinear analysis. The corresponding critical Froude number F_{xc} is given by

$$F_{xc} = \pm(\tanh \lambda h/\lambda h)^{\frac{1}{2}}. \tag{2.12}$$

The long-wave limit ($\lambda h \to 0$) gives the values

$$b_1 = \frac{-\mathrm{i}F_x^2 D}{2(F_x^2-1)} \mathrm{e}^{\mathrm{i}\lambda x} + \text{c.c.}, \tag{2.13a}$$

$$u_1 = \phi_{1c,x} = \frac{\mathrm{i}U_0(D/h)}{2(F_x^2-1)} \mathrm{e}^{\mathrm{i}\lambda x} + \text{c.c.}, \tag{2.13b}$$

which are solutions of the appropriate shallow-water equations

$$U_0 u_{1x} + g b_{1x} = 0, \tag{2.14a}$$

$$\{h u_1 + (b_1 - \delta) U_0\}_x = 0. \tag{2.14b}$$

3. Conditions for Bragg Resonance

The presence of currents has a strong influence on the geometry of the wavenumber triad taking part in the resonant Bragg interaction. Denoting the wavenumber vectors for the incident and reflected waves by $\boldsymbol{k}_1 = (l_1, m_1)$ and $\boldsymbol{k}_2 = (-l_2, m_2)$ (where l_2 is taken positive), respectively, we may write the conditions for three-wave resonance as

$$\boldsymbol{k}_1 - \boldsymbol{\lambda} = \boldsymbol{k}_2, \quad \omega_1 - 0 = \omega_2. \tag{3.1a,b}$$

Equation (3.1b) imposes a uniform frequency on the incident and reflected wave. The wavenumber vector $\boldsymbol{\lambda}$ represents the effect of the bar field. Angles of incidence θ_i with respect to the x-axis are defined according to

$$l_i = |k_i \cos\theta_i| \quad \text{(defined positive)}, \tag{3.2a}$$

$$m_i = k_i \sin\theta_i, \tag{3.2b}$$

$$k_i = |\boldsymbol{k}_i| = (l_i^2 + m_i^2)^{\frac{1}{2}}. \tag{3.2c}$$

The geometry of a resonant triad is indicated in figure 2. Expanding (3.1a) in x- and y-components then gives the conditions

$$l_1 - \lambda = -l_2; \quad \lambda = |\boldsymbol{\lambda}|, \tag{3.3a}$$

$$m_1 = m_2, \tag{3.3b}$$

where (3.3b) represents conservation of wave crests and (3.3a) is the main Bragg condition. The free-wave dispersion relations for each component $\boldsymbol{k}_1, \boldsymbol{k}_2$ may be written as

$$(\omega - k_1 \gamma(\theta_1))^2 = g k_1 \tanh k_1 h, \tag{3.4a}$$

$$(\omega - k_2 \gamma(\theta_2))^2 = g k_2 \tanh k_2 h, \tag{3.4b}$$

where

$$\gamma(\theta) = U_0 \cos\theta + V_0 \sin\theta. \tag{3.5}$$

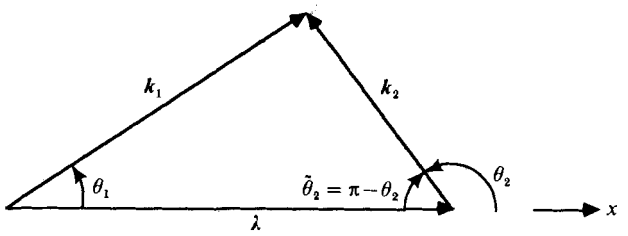

FIGURE 2. Geometry of the three-wave interaction.

We define the two intrinsic frequencies to be

$$\sigma_i = \omega - k_i \gamma(\theta_i). \tag{3.6}$$

The currents U_0 and V_0 are defined to be positive when they flow in the positive sense in each coordinate. We assume that each wave has a positive propagation sense in the y-direction. For later convenience, we define

$$\tilde{\theta}_2 = \pi - \theta_2 \tag{3.7}$$

as the acute angle for the second wave component.

It is clear that $\tilde{\theta}_2$ will not equal θ_1 except in the case of no currents. Further, from (3.3*b*), we require $k_2 > k_1 \sin\theta_1$ for the reflected wave to be freely propagating. For $k_2 = k_1 \sin\theta_1$, the k_2 (reflected) wave field is travelling along the patch in the y-direction. For $k_2 < k_1 \sin\theta_1$, the reflected wave field will be evanescent away from the bar field and hence will be trapped over the bars. This case does not correspond to a resonant case in the sense used below, and its description would require a separate formulation. The limiting conditions corresponding to this case may be directly obtained. We take

$$k_2 = k_1 \sin\theta_1; \quad \theta_2 = \tfrac{1}{2}\pi \tag{3.8}$$

and substitute (3.8) and (3.3*a*) in (3.4) to obtain

$$F_A = \left(\frac{\tan\theta_1}{\lambda h}\tanh(\lambda h \tan\theta_1)\right)^{\frac{1}{2}} - \left(\frac{1}{\lambda h \cos\theta_1}\tanh\left(\frac{\lambda h}{\cos\theta_1}\right)\right)^{\frac{1}{2}}, \tag{3.9}$$

where F_A is the critical value of F_x. In the limiting case of small λh, we obtain directly

$$F_A = \frac{\sin\theta_1 - 1}{\cos\theta_1}. \tag{3.10}$$

Plots of F_A versus θ_1 for a range of λh-values are given in figure 3.

We consider first the case of normal incidence on the bar field. The condition for resonant interaction reduces to

$$k_1 + k_2 = \lambda. \tag{3.11}$$

In the absence of current U_0, (3.11) reduces simply to $2k/\lambda = 1$. Assuming x-direction propagation only and using (3.11) to eliminate k_2 from (3.4*b*) gives the relations

$$(\omega - k_1 U)^2 = g k_1 \tanh k_1 h, \tag{3.12a}$$

$$(\omega + (\lambda - k_1) U)^2 = g(\lambda - k_1)\tanh(\lambda - k_1) h, \tag{3.12b}$$

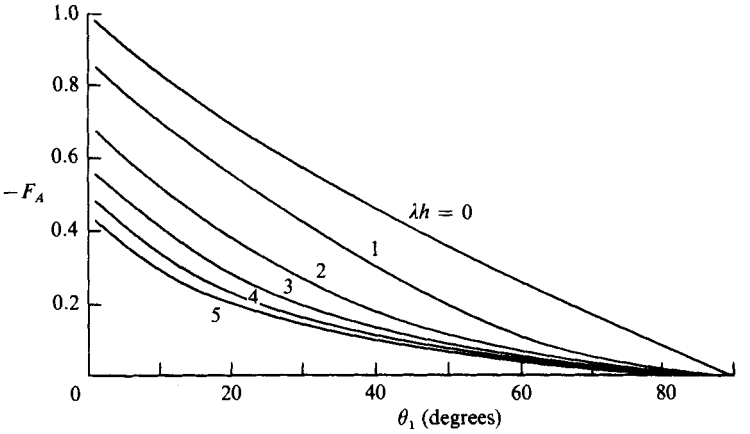

FIGURE 3. Limiting Froude number F_A (3.11) for oblique angle θ_1 of incident wave. $\lambda h = 0$ corresponds to long-wave asymptote.

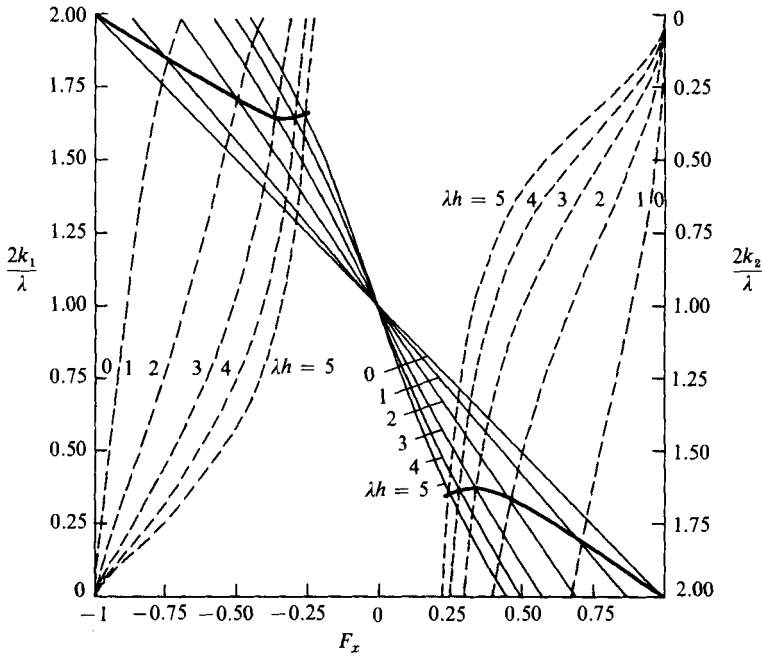

FIGURE 4. Resonant value of $2k_1/\lambda, 2k_2/\lambda$ versus Froude number F_x for various λh-values. Normal incidence. ——, resonance condition; – – –, values of stopping Froude number $F_{s1,2}$ (3.17) for given k_1, k_2; ——, outer envelope of resonant wave conditions involving waves which may propagate to still water.

which in general may be solved numerically for the resonant frequency ω_r and normalized incident wavenumber $(2k_1/\lambda)_r$. The long-wave limit ($\lambda h \to 0$) may be solved directly to obtain

$$\left(\frac{2k_1}{\lambda}\right)_r = 1 - F_x; \quad \left(\frac{2k_2}{\lambda}\right)_r = 1 + F_x, \quad F_x \lesseqgtr 0, \tag{3.13}$$

and the wave frequency at resonance is

$$\omega_r = \tfrac{1}{2}(gh)^{\frac{1}{2}}\lambda(1 - F_x^2). \tag{3.14}$$

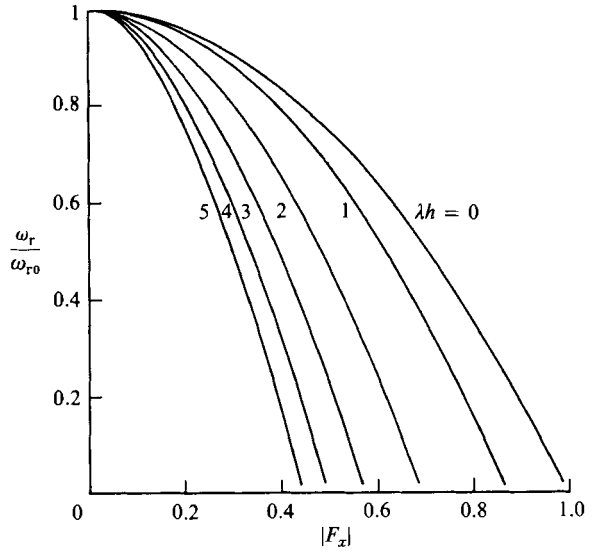

FIGURE 5. Normalized ω_r/ω_{r0} versus F_x for various λh-values. Normal incidence.

Plots of $2k_1/\lambda$ versus F_x are given for values of λh ranging from 0 to 5 in figure 4. (For comparison, λh-values in the experiments of Davies & Heathershaw ranged from 0.79 to 3.14.) For λh-values greater than 5 or 6, the water is effectively deep and the bars have very little influence on the surface waves, unless the current speed is near the resonance condition F_{xc} (2.12). The effect that approaching this condition has on the reflection process is illustrated in §5. The choices of possible ω_r are limited by the restriction that the current should not be a stopping current for either wave component ($C_1, C_2 \neq 0$ in (4.24)), which gives

$$|U| < \frac{\partial \sigma_i}{\partial k_i}; \quad i = 1 \text{ or } 2, \tag{3.15}$$

where the σ_i are given by (3.6) with $\gamma(0) = U_0$. This condition may be written in the notation of this section as

$$|F_x| < F_{s,i} = \frac{1}{2} \frac{\tanh\left[\left(\frac{2k_i}{\lambda}\right)(\frac{1}{2}\lambda h)\right]^{\frac{1}{2}}}{\left(\frac{2k_i}{\lambda}\right)(\frac{1}{2}\lambda h)} \left(1 + \frac{\left(\frac{2k_i}{\lambda}\right)(\lambda h)}{\sinh\left(\frac{2k_i}{\lambda}\right)(\lambda h)}\right), \tag{3.16}$$

where subscript s denotes 'stopping' Froude number. These limits are illustrated by light dashed lines in figure 4 for various choices of λh, in comparison with the curves denoting resonance conditions. The heavy solid curves represent envelopes of possible resonance conditions representing waves which are both free to propagate into or from regions with weaker currents. We note that the interaction curves intersect $2k_1/\lambda = 0, 2$ at the values of the critical Froude number F_{xc} given by (2.12), which represents the case of a stationary wave of wavenumber λ over the bar field. The stopping current conditions $F_{s,i}$ are more stringent for finite depths.

In figure 5, the ratio of resonant frequency ω_r to resonant frequency in the absence of current ω_{r0} is plotted for several λh-values. The decrease in frequency for all λh is symmetric in F_x, as in the shallow-water limit. For relatively large values of

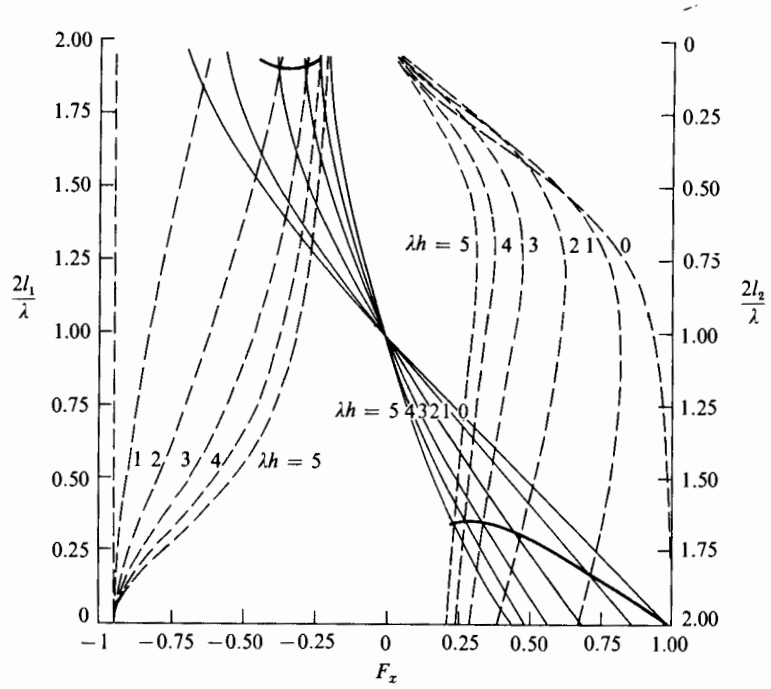

FIGURE 6. Resonant values of $2l_1/\lambda, 2l_2/\lambda$. Oblique incidence, $\theta_1 = 20°$. ——, resonance condition; – – –, stopping Froude numbers $F_{s1,2}$ for given l_1, l_2; ——, envelope of possible resonant conditions.

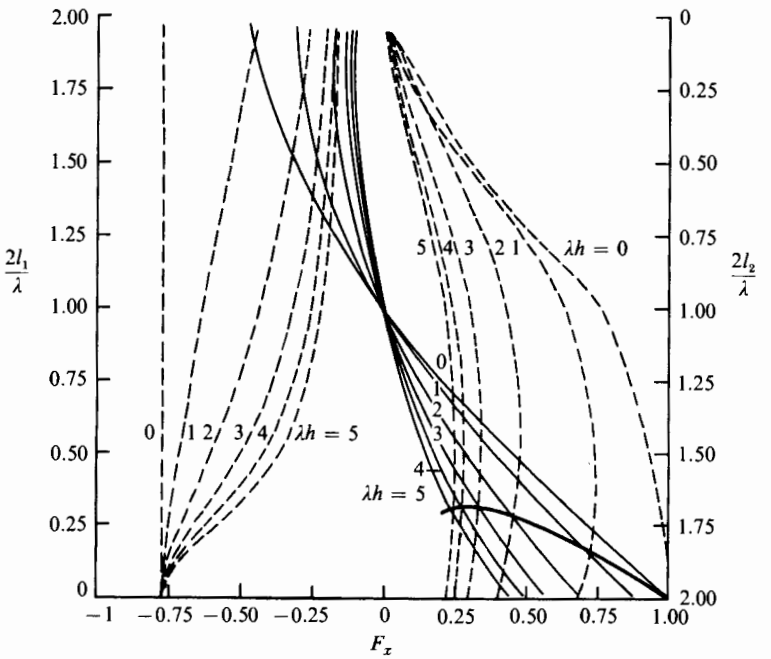

FIGURE 7. As in figure 6. Oblique incidence, $\theta_1 = 40°$.

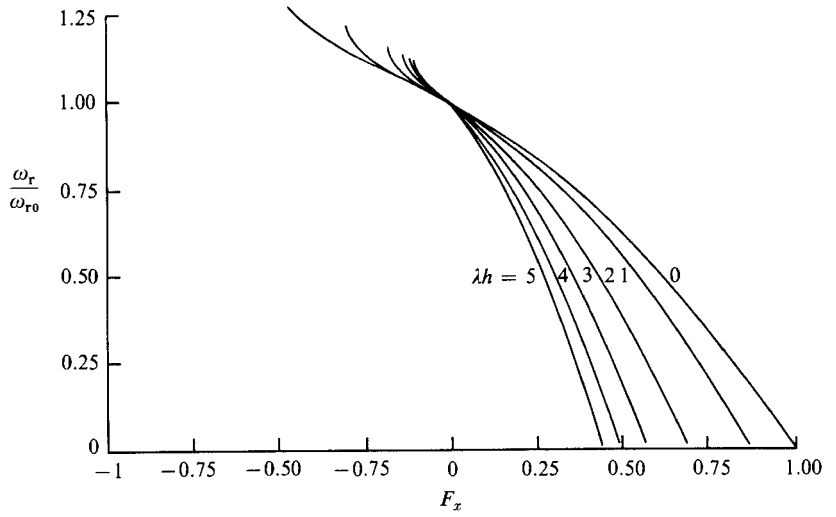

FIGURE 8. Normalized ω_r/ω_{r0} for oblique incidence, $\theta_1 = 40°$.

λh ($\sim$3–5), the decrease in resonant frequency can be quite significant at realizable current values.

Turning to the case of oblique incidence, it becomes necessary to solve the full set of equations (3.3) and (3.4) for the unknown ω_r, $(2k_1/\lambda)_r$, $(2k_2/\lambda)_r$ and θ_2 given λh and angle of incidence θ_1. As before, the shallow-water limit $\lambda h \to 0$ may be solved directly; we obtain the results

$$\left(\frac{2k_1}{\lambda}\right)_r = \frac{(1-F_x^2)}{(F_x+\cos\theta_1)}, \tag{3.17}$$

$$\left(\frac{2k_2}{\lambda}\right)_r = \frac{1+F_x^2+2F_x\cos\theta_1}{(F_x+\cos\theta_1)}, \tag{3.18}$$

$$\omega_r = \frac{(gh)^{\frac{1}{2}}\lambda(1-F_x^2)(1+\cos\theta_1 F_x+\sin\theta_1 F_y)}{2(F_x+\cos\theta_1)}, \tag{3.19}$$

$$\tilde{\theta}_2 = \sin^{-1}\left\{\frac{\sin\theta_1(1-F_x^2)}{1+F_x^2+2F_x\cos\theta_1}\right\}. \tag{3.20}$$

Plots of values of $(2l_1/\lambda)_r$ and $(2l_2/\lambda)_r$ versus F_x are given in figures 6 and 7 for $\theta_1 = 20°$ and $40°$, respectively. The resonance conditions become distinctly asymmetric with respect to currents opposing or following the incident wave. For opposing currents $(2l_1/\lambda) \to 2$ at the limiting value F_A given in (3.9), whereas for following currents the critical condition is still F_{xc}. The value of F_A may also be a more stringent limit than $F_{s,1}$ depending on λh and the angle of incidence. For these plots, we have taken $F_y = 0$. The pronounced asymmetry in the interaction conditions are also strongly apparent in the resonant frequency, which is plotted in figure 8 for the case of $\theta_1 = 40°$.

4. Governing equations for varying wave amplitude

We now consider the problem of reflection linear time-harmonic waves. We drop subscript w in (2.2) and denote the wave velocity potential by ϕ and the surface displacement by η. Expanding the surface boundary conditions about $z = 0$, linearizing in ϕ and η and retaining terms to $O(\epsilon)$ in the undulations (where ϵ simply characterizes the vertical scale of $\delta(x)$), we obtain

$$\nabla_h^2 \phi + \phi_{zz} = 0, \qquad -h \leqslant z \leqslant 0, \quad (4.1)$$

$$\phi_z = \epsilon \nabla_h \cdot (\delta \nabla_h \phi), \qquad z = -h, \quad (4.2)$$

$$\frac{D\eta}{Dt} + \epsilon(u_1 \eta_x + \phi_x b_{1,x}) = \phi_z + \epsilon(b_1 \phi_{zz} + \eta w_{1,z}), \qquad z = 0, \quad (4.3)$$

$$g\eta + \frac{D\phi}{Dt} + \epsilon\left(b_1 \frac{D(\phi_z)}{Dt} + u_1 \phi_x + w_1 \phi_z - g^{-1} U_0 u_{1,z} \frac{D\phi}{Dt}\right) = 0, \quad z = 0, \quad (4.4)$$

where $(u_1, w_1) = \nabla \phi_{1c}$. Also, D/Dt denotes a total derivative following the uniform flow field (U_0, V_0),

$$\frac{D}{Dt} = \frac{\partial}{\partial t} + U_0 \frac{\partial}{\partial x} + V_0 \frac{\partial}{\partial y}. \quad (4.5)$$

Surface displacement η may be eliminated between (4.3)–(4.4) to give a combined surface boundary condition

$$\frac{D^2\phi}{Dt^2} + g\phi_z + \epsilon\left\{\frac{D}{Dt}\left(b_1 \frac{D(\phi_z)}{Dt}\right) + \frac{D}{Dt}(u_1 \phi_x + w_1 \phi_z) - g \nabla_h \cdot (b_1 \nabla_h \phi) + u_1 \frac{D\phi_x}{Dt} - w_{1,z} \frac{D\phi}{Dt} - g^{-1} \frac{D}{Dt}\left(U_0 u_{1,z} \frac{D\phi}{Dt}\right)\right\} = 0, \quad z = 0. \quad (4.6)$$

We introduce the expansions

$$\phi = \phi_0 + \epsilon\phi_1 + \ldots, \quad \eta = \eta_0 + \epsilon\eta_1 + \ldots. \quad (4.7a, b)$$

Anticipating that wave amplitudes will vary over the bar field on a lengthscale commensurate with the interaction effect, we introduce the following multiple scales:

$$x \to x + \epsilon x + \ldots = x + X_1, \quad (4.8a)$$

$$y \to y + \epsilon y + \ldots = y + Y_1, \quad (4.8b)$$

$$t \to t + \epsilon t + \ldots = t + T_1. \quad (4.8c)$$

Substituting (4.7)–(4.8) into (4.1), (4.2) and (4.6) yields the following problems after collecting terms of $O(1)$ and $O(\epsilon)$:

$O(1)$

$$\nabla_h^2 \phi_0 + \phi_{0,zz} = 0, \quad -h \leqslant z \leqslant 0, \quad (4.9a)$$

$$\phi_{0,z} = 0, \qquad z = -h, \quad (4.9b)$$

$$\frac{D^2\phi_0}{Dt^2} + g\phi_{0,z} = 0, \quad z = 0. \quad (4.9c)$$

$O(\epsilon)$

$$\nabla_h^2\phi_1+\phi_{1,zz}=H_1, \qquad -h\leqslant z\leqslant 0, \tag{4.10a}$$

$$\phi_{1,z}=B_1, \qquad z=-h, \tag{4.10b}$$

$$\frac{\mathrm{D}^2\phi_1}{\mathrm{D}t^2}+g\phi_{1,z}=-G_1-G_2, \qquad z=0, \tag{4.10c}$$

where

$$H_1=-2\phi_{0,xX_1}-2\phi_{0,yY_1}, \tag{4.11a}$$

$$B_1=\delta_x\phi_{0,x}+\delta\nabla_h^2\phi_0, \qquad z=-h, \tag{4.11b}$$

$$G_1=2\left(\frac{\mathrm{D}\phi_0}{\mathrm{D}t}\right)_{T_1}+2U_0\left(\frac{D\phi_0}{Dt}\right)_{X_1}+2V_0\left(\frac{D\phi_0}{Dt}\right)_{Y_1}, \qquad z=0, \tag{4.11c}$$

$$\begin{aligned}G_2=&\frac{\mathrm{D}}{\mathrm{D}t}(b_1\phi_{0,zt})-g\nabla\cdot(b_1\nabla_h\phi_0)+\frac{\mathrm{D}}{\mathrm{D}t}(u_1\phi_{0,x}+w_1\phi_{0,z})\\&+\frac{\mathrm{D}}{\mathrm{D}t}(U_0b_1\phi_{0,xz}+V_0b_1\phi_{0,yz})+u_1\frac{\mathrm{D}\phi_{0,x}}{\mathrm{D}t}-w_{1,z}\frac{\mathrm{D}\phi_0}{\mathrm{D}t}\\&-\frac{U_0}{g}\frac{\mathrm{D}}{\mathrm{D}t}\left(u_{1,z}\frac{\mathrm{D}\phi_0}{\mathrm{D}t}\right), \qquad z=0.\end{aligned} \tag{4.11d}$$

Here, G_1 contains slow-scale effects and G_2 contains the influence of the fluctuating current through the surface boundary conditions. We choose ϕ_0 to be of the form

$$\phi_0=\psi^+(X_1,Y_1,T_1;z)\,\mathrm{e}^{\mathrm{i}S_1}+\psi^-(X_1,Y_1,T_1;z)\,\mathrm{e}^{\mathrm{i}S_2}+\text{c.c.}, \tag{4.12}$$

where

$$S_1=l_1x+my-\omega t; \quad S_2=-l_2x+my-\omega t \tag{4.13}$$

represent the phase functions of the incidental and reflected wave, respectively. Substituting (4.12)–(4.13) in (4.9) yields the results

$$\psi^+(X_1,Y_1,T_1;z)=-\tfrac{1}{2}\mathrm{i}gA(X_1,Y_1,T_1)\frac{\cosh k_1(h+z)}{\cosh k_1h}, \tag{4.14a}$$

$$\psi^-(X_1,Y_1,T_1;z)=-\tfrac{1}{2}\mathrm{i}gB(X_1,Y_1,T_1)\frac{\cosh k_2(h+z)}{\cosh k_2h}, \tag{4.14b}$$

where k_1, k_2 and ω are related by (3.4), and where A and B are surface displacement amplitudes divided by intrinsic frequency. We note that the local action densities for each wave train are then proportional to $\sigma_1|A|^2$ and $\sigma_2|B|^2$.

Turning to the $O(\epsilon)$ problem, we write ϕ_1 as

$$\phi_1=\zeta^+(X_1,Y_1,T_1;z)\,\mathrm{e}^{\mathrm{i}S_1}+\zeta^-(X_1,Y_1,T_1;z)\,\mathrm{e}^{\mathrm{i}S_2}+\text{c.c.} \tag{4.15}$$

Following the procedure outlined by Mei (1985), we may decompose B_1, H_1, G_1 and G_2 into $\mathrm{e}^{\mathrm{i}S_1}$ and $\mathrm{e}^{\mathrm{i}S_2}$ components; for example

$$B_1=B_{11}\,\mathrm{e}^{\mathrm{i}S_1}+B_{12}\,\mathrm{e}^{\mathrm{i}S_2}+\text{c.c.} \tag{4.16}$$

Noting that $S_1-S_2=\lambda x$, where $\lambda=l_1+l_2$ at resonance, and recalling that B_1 and G_2 contain rapidly fluctuating terms, we obtain the set of problems

$$\zeta^+_{zz}-k_1^2\zeta^+=H_{11}, \qquad -h\leqslant z\leqslant 0, \tag{4.17a}$$

$$\zeta^+_z=B_{12}\,\mathrm{e}^{-\mathrm{i}\lambda x}, \qquad z=-h, \tag{4.17b}$$

$$\sigma_1^2\zeta^+-g\zeta^+_z=G_{11}+G_{22}\,\mathrm{e}^{-\mathrm{i}\lambda x}, \qquad z=0; \tag{4.17c}$$

and
$$\zeta^-_{zz} - k_2^2 \zeta^- = H_{12}, \qquad -h \leqslant z \leqslant 0, \tag{4.18a}$$
$$\zeta^-_z = B_{11} \, \mathrm{e}^{\mathrm{i}\lambda x}, \qquad z = -h, \tag{4.18b}$$
$$\sigma_2^2 \zeta^- - g\zeta^-_z = G_{12} + G_{21} \, \mathrm{e}^{\mathrm{i}\lambda x}, \quad z = 0. \tag{4.18c}$$

Each problem has the homogeneous solution $\zeta_{\mathrm{H}}^{(+,-)} = \psi^{(+,-)}$, and so solvability conditions are required. Use of Green's second identity on (4.17) and (4.18) separately gives the conditions

$$\int_{-h}^{0} \psi^+ H_{11} \, \mathrm{d}z + \frac{1}{g}(G_{11} + G_{22} \, \mathrm{e}^{-\mathrm{i}\lambda x}) \psi^+(0) + B_{11} \, \mathrm{e}^{-\mathrm{i}\lambda x} \psi^+(-h) = 0, \tag{4.19a}$$

$$\int_{-h}^{0} \psi^- H_{12} \, \mathrm{d}z + \frac{1}{g}(G_{12} + G_{21} \, \mathrm{e}^{\mathrm{i}\lambda x}) \, \psi^-(0) + B_{12} \, \mathrm{e}^{\mathrm{i}\lambda x} \psi^-(-h) = 0. \tag{4.19b}$$

Substituting for the inhomogeneous terms then gives the following set of evolution equations for A and B:

$$\frac{\sigma_1}{\omega}\{A_{T_1} + (Cg_1 \cos\theta_1 + U_0) A_{X_1} + (Cg_1 \sin\theta_1 + V_0) A_{Y_1}\} = -\Omega_{\mathrm{c}} B, \tag{4.20a}$$

$$\frac{\sigma_2}{\omega}\{B_{T_1} + (-Cg_2 \cos\tilde{\theta}_2 + U_0) B_{X_1} + (Cg_2 \sin\tilde{\theta}_2 + V_0) B_{Y_1}\} = \Omega_{\mathrm{c}} A. \tag{4.20b}$$

The interaction coefficient Ω_{c} is given by

$$\Omega_{\mathrm{c}} = \Omega_{0\mathrm{c}} \cos(\theta_1 + \tilde{\theta}_2) + \Omega_{1\mathrm{c}}, \tag{4.21}$$

where
$$\Omega_{0\mathrm{c}} = \frac{gk_1 k_2 D}{4\omega \cosh k_1 h \cosh k_2 h}, \tag{4.22a}$$

$$\Omega_{1\mathrm{c}} = (4\omega\alpha \cosh\lambda h)^{-1}\{\lambda U_0(l_2\sigma_1 - l_1\sigma_2) D - \frac{\lambda U_0^2}{g}[gk_1 k_2 \cos(\theta_1 + \tilde{\theta}_2) + \frac{\sigma_1\sigma_2}{g}(\sigma_1\sigma_2 + (\lambda U_0)^2)]\, D\}, \tag{4.22b}$$

where α is given by (2.11a). In the absence of currents, $\Omega_{1\mathrm{c}} = 0$ and

$$\Omega_{\mathrm{c}} \to \frac{gk^2 D}{4\omega \cosh^2 kh} \cos 2\theta = \frac{g\lambda^2 D}{16\omega \cosh^2(\frac{1}{2}\lambda h)} \cos 2\theta, \tag{4.23}$$

and the evolution equations given by Mei (1985) are recovered after taking $\sigma_1 = \sigma_2 = \omega$ and converting to surface displacement amplitudes.

For the special case of normal incidence ($\partial/\partial y = 0$), (4.20) may be reduced to the form

$$A_{T_1} + C_1 A_{X_1} = -\frac{\Omega_{\mathrm{c}}\omega}{\sigma_1} B, \tag{4.24a}$$

$$B_{T_1} - C_2 B_{X_1} = \frac{\Omega_{\mathrm{c}}\omega}{\sigma_2} A, \tag{4.24b}$$

where
$$C_1 = Cg_1 + U_0; \quad C_2 = Cg_2 - U_0 \tag{4.25a,b}$$

These equations may be rearranged to read

$$\begin{pmatrix} A \\ B \end{pmatrix}_{T_1 T_1} + \Delta \begin{pmatrix} A \\ B \end{pmatrix}_{X_1 T_1} - C_1 C_2 \begin{pmatrix} A \\ B \end{pmatrix}_{X_1 X_1} + (\Omega_{\mathrm{c}}')^2 \begin{pmatrix} A \\ B \end{pmatrix} = 0, \tag{4.26}$$

where
$$\Delta = C_1 - C_2, \tag{4.27}$$
$$(\Omega_c')^2 = \frac{\Omega_c^2 \omega^2}{\sigma_1 \sigma_2}. \tag{4.28}$$

These equations differ in form from the Klein–Gordon equations obtained in the no-current case; however, a phase shift introduced in A and B will lead to solutions with forms similar to those obtained by Mei.

Alternately, (4.24) may be arranged in the form
$$\{\sigma_1|A|^2 + \sigma_2|B|^2\}_{T_1} + \{\sigma_1|A|^2 C_1 - \sigma_2|B|^2 C_2\}_{X_1} = 0, \tag{4.29}$$
which indicates conservation of wave action during the reflection process.

5. Normally incident waves over a finite bar field

We now consider a periodic wave train propagating from $x \sim -\infty$ over a bar field located in the spatial interval $0 \leqslant x \leqslant L$. We take $l = 2\pi/\lambda$ to be the bar wavelength and require $L = nl$, where n is an integer $\geqslant 1$. The waves are assumed to be normally incident ($\theta_1 = \tilde{\theta}_2 = 0, l_1 = k_1, l_2 = k_2, \partial/\partial y \equiv 0$). The resonant wave frequency is taken to be ω_r, and the wave train is allowed to have a slightly detuned frequency $\omega = \omega_r + \epsilon\Omega$. (We retain Mei's notation as far as possible in this section in order to facilitate comparisons.) The corresponding detuned wavenumbers are then
$$k_1 + \epsilon K_1; \quad \Omega = C_1 K_1, \tag{5.1a}$$
$$k_2 + \epsilon K_2; \quad \Omega = C_2 K_2. \tag{5.1b}$$

5.1. *The solutions for periodic wave trains*

In the region upwave of the patch, the homogeneous solutions to (4.26) are given by
$$A = A_0 \, e^{i(K_1 x - \Omega t)}; \qquad x < 0, \tag{5.2a}$$
$$B = B_0 \, e^{i(-K_2 x - \Omega t)}; \qquad x < 0. \tag{5.2b}$$

Downwave of the patch, we require $B(x > L) = 0$ representing no wave arriving from $x \sim \infty$. Boundary conditions consist of continuity requirements on A and B at $x = 0, L$. Over the bar field, we introduce the forms
$$A(x,t) = \hat{A}(x) \, e^{-i\Omega t}; \quad B(x,t) = \hat{B}(x) \, e^{-i\Omega t}. \tag{5.3}$$

Introduction of (5.3) in (4.26) then gives
$$\begin{pmatrix} \hat{A} \\ \hat{B} \end{pmatrix}_{xx} + i\Theta \begin{pmatrix} \hat{A} \\ \hat{B} \end{pmatrix}_x + (P')^2 \begin{pmatrix} \hat{A} \\ \hat{B} \end{pmatrix} = 0, \tag{5.4}$$

where
$$\Theta = \Delta\Omega (C_1 C_2)^{-1}, \tag{5.5}$$
$$(P')^2 = (C_1 C_2)^{-1}(\Omega^2 - (\Omega_c')^2). \tag{5.6}$$

A final substitution gives equations analogous to Mei's; let
$$\hat{A}(x) = \tilde{A}(x) \, e^{-i\Theta x/2}; \quad \hat{B}(x) = \tilde{B}(x) \, e^{-i\Theta x/2} \tag{5.7}$$

to obtain
$$\begin{pmatrix} \tilde{A} \\ \tilde{B} \end{pmatrix}_{xx} + P^2 \begin{pmatrix} \tilde{A} \\ \tilde{B} \end{pmatrix} = 0, \tag{5.8}$$

where
$$P^2 = (P')^2 + \tfrac{1}{4}\Theta^2. \tag{5.9}$$

A value of Ω corresponding to a cutoff condition may be found by determining the zero of P^2; the resulting condition is

$$\Omega^2_{\text{cutoff}} = \frac{(\Omega'_c)^2}{\left(1+\dfrac{\Delta^2}{4C_1C_2}\right)}. \tag{5.10}$$

In the absence of currents, the cutoff frequency is given by $\pm\Omega_0$ as in Mei. We examine the four corresponding cases.

Case 1. $P^2 > 0$ (*frequency above cutoff*)

The solutions to (5.8) and hence (4.28) are found to be

$$A(x,t) = A_0\, e^{-i\Theta x/2}\frac{\{PC_1\cos P(L-x) - i\Omega'\sin P(L-x)\}}{\{PC_1\cos PL - i\Omega'\sin PL\}}e^{-i\Omega t}, \tag{5.11}$$

$$B(x,t) = \frac{A_0\, e^{-i\Theta x/2}\Omega'_c\left(\dfrac{\sigma_1}{\sigma_2}\right)^{\frac{1}{2}}\left(\dfrac{C_1}{C_2}\right)\sin P(L-x)}{[PC_1\cos PL - i\Omega'\sin PL]}e^{-i\Omega t}, \tag{5.12}$$

where
$$\Omega' = \Omega + \tfrac{1}{2}C_1\Theta. \tag{5.13}$$

The reflected and transmitted wave intensities are oscillatory over the bar field and also oscillate with bar-field length.†

Case 2. $P^2 = 0$ (*cutoff frequency*)

We obtain

$$A(x,t) = A_0\, e^{-i\Theta x/2}\frac{(1-i(\Omega'/C_1)(L-x))}{1-i\Omega'L/C_1}e^{-i\Omega t}, \tag{5.14}$$

$$B(x,t) = A_0\, e^{-i\Theta x/2}\frac{\Omega'_c(\sigma_1/\sigma_2)^{\frac{1}{2}}(C_2^{-1})(L-x)}{1-i\Omega'L/C_1}e^{-i\Omega t}. \tag{5.15}$$

Case 3. $P^2 < 0$ (*frequency below cutoff*)

We take
$$Q = iP \tag{5.16}$$

and obtain

$$A(x,t) = A_0\, e^{-i\Theta x/2}\frac{\{QC_1\cosh Q(L-x) + i\Omega'\sinh Q(L-x)\}}{\{QC_1\cosh QL + i\Omega'\sinh QL\}}e^{-i\Omega t}, \tag{5.17}$$

$$B(x,t) = -A_0\, e^{-i\Theta x/2}\frac{\Omega'_c(\sigma_1/\sigma_2)^{\frac{1}{2}}(C_1/C_2)\sinh Q(L-x)}{\{QC_1\cosh QL + i\Omega'\sinh QL\}}e^{-i\Omega t}. \tag{5.18}$$

Case 4. $\Omega = 0$ (*perfect tuning*)

The coefficient Q^2 from (5.16) reduces to

$$Q^2 = (\Omega'_c)^2(C_1C_2)^{-1}. \tag{5.19}$$

We obtain the results

$$A(x,t) = A(x) = A_0\frac{\cosh Q(L-x)}{\cosh QL}, \tag{5.20}$$

$$B(x,t) = B(x) = -A_0\left(\frac{\sigma_1}{\sigma_2}\right)^{\frac{1}{2}}\left(\frac{C_1}{C_2}\right)^{\frac{1}{2}}\frac{\sinh Q(L-x)}{\cosh QL}. \tag{5.21}$$

† We note that the reflected waves given here differ in phase by 45° from Mei's results; this stems from his choosing bottom modulation $\phi = D\cos\lambda x$ and starting the patch at $x = 0$. The approach used here ($\phi \sim \sin\lambda x$) represents a continuous bottom.

The reflection coefficient is given by

$$\frac{|B(0)|}{A_0} = \left(\frac{\sigma_1}{\sigma_2}\right)^{\frac{1}{2}} \left(\frac{C_1}{C_2}\right)^{\frac{1}{2}} \tanh QL. \tag{5.22}$$

Note that as $L \to \infty$, the reflection coefficient differs from unity owing to wave–current effects.

We note that the solutions for cases 1–4 all satisfy the condition

$$\sigma_1 A_0^2 C_1 - \sigma_2 |B(0)|^2 C_2 = \sigma_1 |A(L)|^2 C_1, \tag{5.23}$$

which represents conservation of action flux during the reflection process, as follows from (4.29).

5.2. *Effect of currents on transmission over the bar field*

We now consider the effect of introducing a current on the reflection–transmission process. In order to simplify the discussion as much as possible, we shall consider effects only at or close to exactly tuned resonance. Further, all comparisons will be based on transmission coefficients in order to avoid the problem of intrinsic-frequency effects in the definitions of the incident and reflected wave action flux. Two examples are considered.

Example 1. *Effect of current on transmission at resonance*

We first consider the effect of a current on the magnitude of transmission past a bar field of length L. The reflection process with or without currents is assumed to be perfectly tuned, and thus the wave frequency is assumed to adjust as the current speed changes, in order to maintain resonance.

Considering the result for $\Omega = 0$, we obtain

$$\left\{\frac{A(L)}{A_0}\right\}_{\text{current}} = (\cosh Q_c L)^{-1}, \tag{5.24}$$

$$\left\{\frac{A(L)}{A_0}\right\}_{\text{no current}} = (\cosh QL)^{-1}, \tag{5.25}$$

where

$$Q = \frac{\Omega_0}{Cg}; \quad Q_c = \frac{\Omega_c'}{(C_1 C_2)^{\frac{1}{2}}} \tag{5.26a,b}$$

The ratio of transmission with current to transmission with no current is then given by

$$T_A = \left|\frac{A(L)_{\text{current}}}{A(L)_{\text{no current}}}\right| = \frac{\cosh QL}{\cosh Q_c L}. \tag{5.27}$$

For the special case of the long-wave limit, all relative phase and group velocities $\to (gh)^{\frac{1}{2}}$, and we obtain

$$Q \to \frac{\lambda D}{8h}; \qquad QL = \frac{n\pi D}{4h}, \tag{5.28}$$

$$Q_c \to \frac{\lambda D}{8h}(1 - F_x^2)^{-1}; \quad Q_c L = \frac{n\pi D}{4h}(1 - F_x^2)^{-1}, \tag{5.29}$$

where n is the number of bars. Note that Q_c has a singularity at $|F_x| \to 1$, which corresponds to the stopping condition for either the incident or reflected wave. For

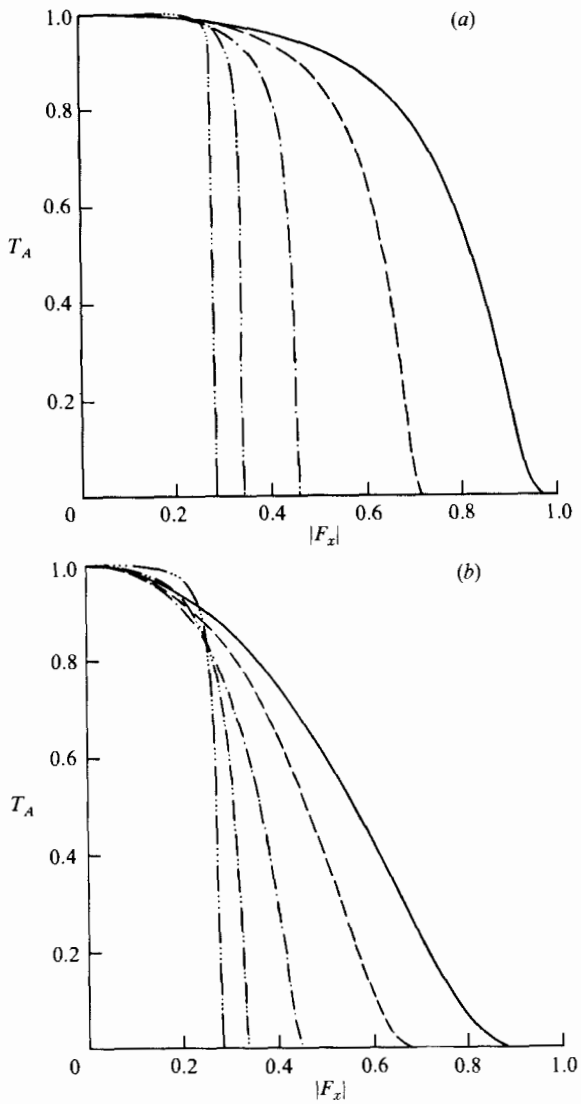

FIGURE 9. Ratio of transmission coefficient without current. Normal incidence, frequency held at resonant value. (*a*) $n = 2, D/h = 0.3$; (*b*) $n = 10, D/h = 0.2$. ——, $\lambda h = 0$; – – –, 1; —·—, 2; —··—, 3; —···—, 4.

$|F_x| < 1$, we have $Q_c > Q$ and hence the ratio of transmission coefficients is less than unity for $F_x \neq 0$. This result indicates that the reflection process is enhanced by the presence of a current as long as resonance conditions are maintained, owing to the additional interaction effects introduced through the surface boundary conditions.

Results for two cases ($n = 2, D/h = 0.3$; $n = 10, D/h = 0.2$) are presented in figure 9 for $\lambda h = 1, 2, 3, 4$ and the long-wave limit. The ratio T_A is symmetric in F_x and drops to zero (representing a singularity in the interaction) when $|F_x|$ goes to the stopping condition F_s predicted by (3.17). (For larger values of λh, coupling is weak and T_A is affected mainly by the singularity at F_s.) In all cases, the presence of a current of arbitrary sign reduces transmission at resonance, and it may therefore be concluded that wave–current interaction uniformly enhances resonant reflection of normally incident waves.

Example 2. *Deviation from resonance at fixed frequency*

We now consider the case where a wave frequency ω_{r0} is chosen by the resonance condition in the absence of currents:

$$\omega_{r0}^2 = \tfrac{1}{2}g\lambda \tanh \tfrac{1}{2}\lambda h. \tag{5.30}$$

The wave field is then assumed to maintain this fixed absolute frequency as the current speed varies from zero, leading to detuning. We thus consider how the magnitude of transmission varies as resonant conditions established for one set of parameters are detuned owing to a shift to another set of parameters. For any given non-zero current speed, the detuning frequency is given by

$$\omega_{r0} = \omega_r + \Omega, \tag{5.31}$$

where ω_r is determined from (3.3)–(3.4). The behaviour of the detuned envelope over the bar field may then take on any of the Case 1–4 behaviours depending on the size of Ω relative to the cutoff frequency predicted by (5.10). Again, we investigate this case in the limit $\lambda h \to 0$ before presenting graphical results.

Substituting long-wave values into (5.10) gives the cutoff condition as

$$\Omega_{\text{cutoff}}^2(\lambda h \to 0) = \frac{g^2\lambda^2 D^2}{64C^2}; \quad C^2 = gh. \tag{5.32}$$

The detuning frequency is given by (5.31):

$$\Omega^2 = \tfrac{1}{4}C^2\lambda^2 F_x^4, \tag{5.33}$$

and hence the cutoff condition is met by introducing a current with magnitude

$$F_x^4 = \left(\frac{D}{4h}\right)^2. \tag{5.34}$$

For example, for $h = 2$ m and a bar height $D/h = 0.2$, a current with $F_x^2 = 0.05$ or velocity $= \pm 1.00$ m/s would be sufficient to shift the parameter Ω to just above the cutoff condition. These conditions would not be unreasonable in the nearshore environment.

Two computational examples corresponding to ($n = 2, D/h = 0.3$) and ($n = 10$, $D/h = 0.2$) are plotted in figure 10 for $\lambda h = 1$, 2, 3, 4 and the long-wave limit. The case with two bars represents a weakly tuned system with a broad and weak resonant-reflection peak (see, for example, figure 6*c* in Davies & Heathershaw 1984). Consequently, transmission coefficients for tuned and untuned cases are close to unity and variations with Froude number F_x are thus weak. In contrast, the case ($n = 10, D/h = 0.2$) represents a sharply tuned system with a narrow, strong resonant-reflection peak (see figure 6*a* in Davies & Heathershaw or figure 2 in Kirby 1986). In the neighbourhood of the resonant peak, the transmission coefficient drops significantly below unity and only rises close to unity in the regions beyond the cutoff condition, touching unity at zeros of the reflection.

The form of T_A, defined initially in (5.27) as $T_A = |A(L)_{\text{current}}/A(L)_{\text{no current}}|$, will change according to which of (5.11), (5.14) or (5.17) is the appropriate solution. We expect $T_A = 1$ at $F_x = 0$, and $T_A \to \cosh QL$ far from resonance. The numerical results indicate this trend. For values of F_x close to zero (Ω below cutoff), the results show a possibly unexpected drop in T_A below unity, indicating that reflection is increasing slightly, even as detuning increases, owing to the significant additional wave–current

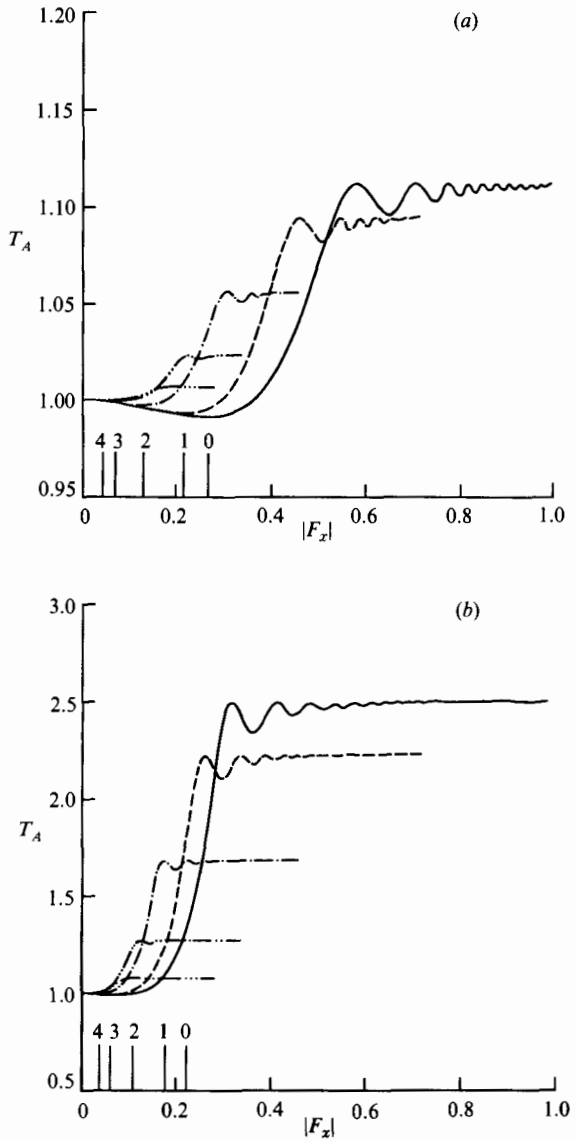

FIGURE 10. Ratio of transmission coefficient with current to transmission coefficient without current. Normal incidence, frequency constant (resonance at $F_x = 0$). Curve labels as in figure 9. Vertical bars denote (F_x) associated with cutoff; labels are λh-values. (*a*) $n = 2, D/h = 0.3$; (*b*) $n = 10, D/h = 0.2$.

effect. As F_x increases (and Ω goes through cutoff), T_A increases and finally approaches $\cosh QL$ in a damped oscillatory fashion. Values of F_x corresponding to cutoff conditions are indicated by vertical bars in figure 10.

6. Oblique wave incidence

We now briefly consider the case of waves arriving at the bar field with angle of incidence θ_1, and provide sufficient information to construct solutions following §5.

We rewrite the governing equations (4.20) as

$$A_t + C_{1x}A_x + C_{1y}A_y = -\Omega_c\left(\frac{\omega}{\sigma_1}\right)B, \tag{6.1a}$$

$$B_t - C_{2x}B_x + C_{2y}B_y = \Omega_c\left(\frac{\omega}{\sigma_2}\right)A, \tag{6.1b}$$

where
$$C_{1x} = Cg_1\cos\theta_1 + U_0, \quad C_{1y} = Cg_1\sin\theta_1 + V_0, \tag{6.2a,b}$$

$$C_{2x} = Cg_2\cos\tilde{\theta}_2 - U_0, \quad C_{2y} = Cg_2\sin\tilde{\theta}_2 + V_0. \tag{6.2c,d}$$

Upwave of the bar field ($x < 0$) and assuming that incident wave modulations propagate in the same direction as the carrier wave, we may write homogeneous solutions of (6.1) in the form

$$A = A_0\exp[\mathrm{i}(K_1\cos\theta_1 x + K_1\sin\theta_1 y - \Omega t)], \tag{6.3a}$$

$$B = B_0\exp[\mathrm{i}(-K_2\cos\theta_2' x + K_2\sin\theta_2' y - \Omega t)], \tag{6.3b}$$

where
$$\Omega = K_1C_{1x}\cos\theta_1 + K_1C_{1y}\sin\theta_1, \tag{6.4a}$$

$$\Omega = K_2C_{2x}\cos\theta_2' + K_2C_{2y}\sin\theta_2', \tag{6.4b}$$

and where we require
$$K_1\sin\theta_1 = K_2\sin\theta_2' = M \tag{6.5}$$

owing to wave-crest conservation. Note that θ_2' differs from $\tilde{\theta}_2$, since the wavenumber vector for the reflected wave will tend to rotate as frequency shifts away from the resonant value. Equations (6.4)–(6.5) are used to determine K_1, K_2 and θ_2' after determination of the resonant-interaction condition.

Following §5, we let

$$\begin{pmatrix} A \\ B \end{pmatrix} = \begin{pmatrix} \tilde{A}(x) \\ \tilde{B}(x) \end{pmatrix} \mathrm{e}^{\mathrm{i}(My - \Omega t - \hat{\Theta}x/2)} \tag{6.6}$$

over the bar field and obtain
$$\begin{pmatrix} \tilde{A} \\ \tilde{B} \end{pmatrix}_{xx} + \hat{P}^2\begin{pmatrix} \tilde{A} \\ \tilde{B} \end{pmatrix} = 0, \tag{6.7}$$

where
$$\hat{P}^2 = \frac{\Omega_1\Omega_2 - (\Omega_c')^2}{C_{1x}C_{2x}} + \tfrac{1}{4}\hat{\Theta}^2, \tag{6.8a}$$

$$\hat{\Theta} = \frac{C_{1x}\Omega_2 - C_{2x}\Omega_1}{C_{1x}C_{2x}}, \tag{6.8b}$$

$$\Omega_1 = \Omega - MC_{1y}, \tag{6.8c}$$

$$\Omega_2 = \Omega - MC_{2y}. \tag{6.8d}$$

The cutoff condition is determined from the equation

$$\Omega^2\left[1 + \frac{(\Delta^x)^2}{4C_{1x}C_{2x}}\right] - (\tfrac{1}{2}M)\,G_1 + (\tfrac{1}{2}M)^2G_2 = (\Omega_c')^2, \tag{6.9}$$

where
$$\Delta^x = C_{1x} - C_{2x}, \tag{6.10}$$

$$G_1 = C_{1y} + C_{2y} + \frac{((C_{1x})^2C_{2y} + (C_{2x})^2C_{1y})}{C_{1x}C_{2x}}, \tag{6.11}$$

$$G_2 = \frac{(C_{1x}C_{2y} + C_{2x}C_{1y})^2}{C_{1x}C_{2x}}. \tag{6.12}$$

These results are sufficient to determine the solutions for $\tilde{A}(x)$, $\tilde{B}(x)$ from (5.11)–(5.21) after substituting $(\hat{P}, \hat{Q}, C_{1x}, \hat{\Omega}', \hat{\Theta})$ for $(P, Q, C_1, \Omega', \Theta)$, where

$$\hat{Q} = \mathrm{i}\hat{P}, \tag{6.13}$$

$$\hat{\Omega}' = \Omega - MC_{1y} + \tfrac{1}{2}C_{1x}\hat{\Theta}. \tag{6.14}$$

7. Discussion

The presence of an ambient current field has been shown to have non-trivial effects on the reflective characteristics of a submerged bar field. The presence of a current flowing offshore over the bar field, opposing the incident wave, is shown to place significant limitations on the geometry of resonant wave triads, which are possible when the incident wave is oblique to the bar field.

Application of the present results in realistic field situations requires the development of an equivalent theory for waves in a slowly varying domain, which would give appropriate extension to the evolution equation (4.20). This extension is being investigated separately in the context of arbitrarily varying domains and the parabolic approximation, and will be reported shortly.

This work was supported by the Office of Naval Research through contract number N00014-86-K-0790. Conversations with J. A. Bailard, R. T. Guza and D. M. Hanes were instrumental in sparking interest in this problem.

REFERENCES

Davies, A. G. & Heathershaw, A. D. 1984 Surface-wave propagation over sinusoidally varying topography. *J. Fluid Mech.* **144**, 419–443.

Hara, T. & Mei, C. C. 1987 Bragg scattering of surface waves by periodic bars: theory and experiment. *J. Fluid Mech.* **178**, 221–241.

Kennedy, J. F. 1963 The mechanics of dunes and antidunes in erodible-bed channels. *J. Fluid Mech.* **16**, 521–544.

Kirby, J. T. 1986 A general wave equation for waves over rippled beds. *J. Fluid Mech.* **162**, 171–186.

Mei, C. C. 1969 Steady free surface flow over a wavy bed. *ASCE J. Engng Mech. Div.* **95**, 1393–1402.

Mei, C. C. 1985 Resonant reflection of surface water waves by periodic sand bars. *J. Fluid Mech.* **152**, 315–335.

Reynolds, A. J. 1965 Waves on the erodible bed of an open channel. *J. Fluid Mech.* **22**, 113–133.